Electronic Supplementary Information

Highly Fluorescent Pyridine-Ended Y6 Derivative as Third Component for Organic Solar Cells

Yu Qiao,[a,b,#] Xuan Liu,[a,#] Yang Li,[a,b] Xin Guo[a,*] and Can Li[a,b,*]

[a] State Key Laboratory of Catalysis, Dalian National Laboratory for Clean Energy, Dalian Institute of Chemical Physics, Chinese Academy of Sciences, Zhongshan Road 457, Dalian, 116023 (China).
[b] University of Chinese Academy of Sciences, Beijing, 100049 (China).
* Corresponding author: guoxin@dicp.ac.cn; canli@dicp.ac.cn

Experimental Section

Materials and methods

Chemicals and solvents were purchased from Nanjing Zhiyan Technology Co., Ltd, Solarmer Materials Inc., or Alfa Aesar. All chemicals were used without further purification.

^{1}H NMR and ^{13}C NMR spectra were obtained on a Bruker AVANCE III 400 MHz spectrometer in $CDCl_3$. The mass spectroscopy (MS) was carried out on ABI MALDI TOF/TOF 5800 using DHB as matrix. UV-vis absorption spectra were measured on a Cary 5000 UV-VIS-NIR spectrophotometer. The photoluminescence spectra were recorded on a QM400 fluorescence spectrometer. The cyclic voltammetry (CV) was conducted on a CHI600E electrochemical workstation in a three-electrode cell in anhydrous acetonitrile solution of tetrabutylammonium hexafluorophosphate (0.1 M) with a scan rate of 50 mV s^{-1} at room temperature. The glassy carbon electrode, Pt wire and Ag/AgCl were used as the working electrode, counter electrode, and reference electrode, respectively. And Ferrocene/Ferrocenium (Fc/Fc^{+}) redox couple was used as the inner reference. Contact angles of films were measured on a Kruss DSA100 instrument. The surface energy (γ) values were calculated by Owens-Wendt method:

$$(\gamma_s^d\gamma_l^d)^{1/2} + (\gamma_s^p\gamma_l^p)^{1/2} = \frac{1}{2}\gamma_l\ (1 + \cos\ \theta) \quad (1)$$

where γ_l is the surface energy of measuring liquids, γ_s is the surface energy of measuring materials, γd and γp are the dispersion and polar components. The steady-state photoluminescent spectra, time-resolved photoluminescence and photoluminescence quantum yield (PLQY) values were all recorded on the Steady/Transient State Fluorescence Spectrometer (FLS 1000, Edinburgh Instruments, UK).

AFM height images were obtained on a Bruker Metrology Nanoscope III-D atomic force microscopy in tapping mode. GIWAXS measurements were performed using the beamline BL14B1 of the Shanghai Synchrotron Radiation Facility (SSRF) with the incident photon energy of 10 keV (wavelength of 1.24 angstrom) at an incident angle of 0.13° and an exposure time of 60 s. The samples for the GIWAXS measurements were prepared by spin-coating solutions on Si substrates.

The trap state densities of the blends were measured using the space-charge-limited current (SCLC) method with the electron-only device architecture of ITO/ZnO/active layer/PDINO/Al. The charge mobilities were measured using the SCLC method with the electron-only device architecture of ITO/ZnO/active layer/PDINO/Al and hole-only device architecture of ITO/PEDOT:PSS/active layer/MoO_3/Al. The J-V curves were measured using the solar simulator (Enlitech, Taiwan) equipped with a Keithley 2400 source-measure unit under illumination (AM 1.5G, 100 mW cm^{-2}) and calibrated with a standard silicon solar cell. The external quantum efficiency (EQE) measurements were performed by the solar cell spectral response measurement system (QE-R, Enlitech). The EQE_{EL} was recorded on the Electroluminescence Efficiency Measurement System (XP-EQE-Adv, Xi Pu Guang Dian, CHN).

The calculations of molecular configuration optimization and dipole moments were conducted using the Gaussian 09 program based on the density functional theory method at the B3LYP/6-31G (d) level.

Device Fabrication and measurement

The structure of OSCs on the glass substrate was ITO/PEDOT:PSS/active layer/PDINO/Ag. The prepatterned ITO-coated glass substrates were cleaned by

sonication with deionized water, isopropyl alcohol, and ethanol sequentially, and then they were treated with UV-ozone for 20 min after drying. The PEDOT:PSS (4083) layer was spin-coated onto the precleaned ITO surface. Subsequently, PEDOT:PSS films were baked at 150 °C for 15 min in the air and then transferred to a nitrogen filled glove box. The active layer materials were dissolved in chloroform, and the total concentration of the solution was 15 mg mL^{-1} (0.5% 1-chloronaphthalene, v/v). The active layer was spin-cast at 3000 rpm for 30 s onto the PEDOT:PSS layer and baked at 90 °C for 10 min. Then, PDINO in methanol solution (1.8 mg mL^{-1}) was spin-coated at 4000 rpm for 30 s. Finally, a 100 nm Ag cathode was thermally evaporated under vacuum at 1×10^{-4} Pa. The device area was 0.04 cm^2.

Synthesis of BTP-N

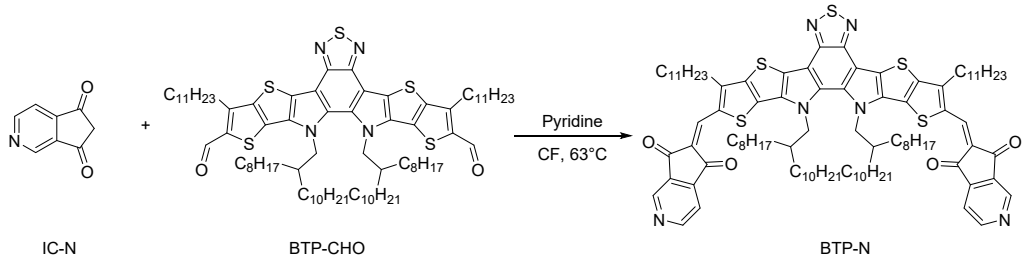

BTP-CHO (136 mg, 0.1 mmol), IC-N (88 mg, 0.6 mmol), pyridine (1 mL) and chloroform (20 mL) were dissolved in a round bottom flask under nitrogen. The mixture was stirred at 70 °C for 48h. After cooling to room temperature, the mixture was poured into methanol and filtered. The residue was purified with column chromatography on silica gel using dichloromethane/ethyl acetate (4/1, v/v) as the eluent to give a dark blue solid BTP-N (79 mg, 49%). ^{1}H NMR: (400 MHz, $CDCl_3$, δ): 9.27 (s, 2H), 9.08 (s, 2H), 8.37 (s, 2H), 7.97 (s, 2H), 4.78 (d, 4H), 3.23 (t, 4H), 2.10 (m, 4H), 1.91 (m, 4H), 1.74 (m, 16H), 1.52 (m, 18H), 1.38 (m, 16H), 0.97 (m, 32H), 0.81 (m, 32H). ^{13}C NMR: (101 MHz, $CDCl_3$, δ): 147.52, 144.73, 137.50, 137.42, 133.90, 132.98, 130.92, 128.85, 113.28, 65.58, 55.56, 39.07, 31.92, 30.93, 30.58, 30.45, 29.83, 29.74, 29.70, 29.67, 29.62, 29.59, 29.56, 29.54, 29.43, 29.41, 29.38, 29.35, 29.32, 25.49, 22.70, 22.68, 19.19, 14.12, 13.74. HR-MS (MALDI-TOF): m/z calcd. for ($C_{98}H_{136}N_6O_4S_5$): 1622.4912. Found: 1622.1443.

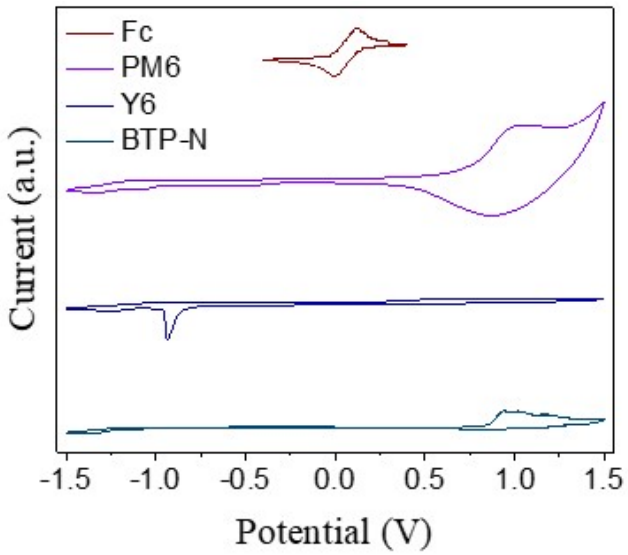

Figure S1. Cyclic voltammetry (CV) curves of PM6, Y6 and BTP-N. The HOMO and LUMO energy levels were determined by E_{HOMO}=-(E_{onset}^{ox}-E_{Fc}+4.8) (eV) and E_{LUMO}=-(E_{onset}^{red}-E_{Fc}+4.8) (eV); E_{Fc}=0.06 eV.

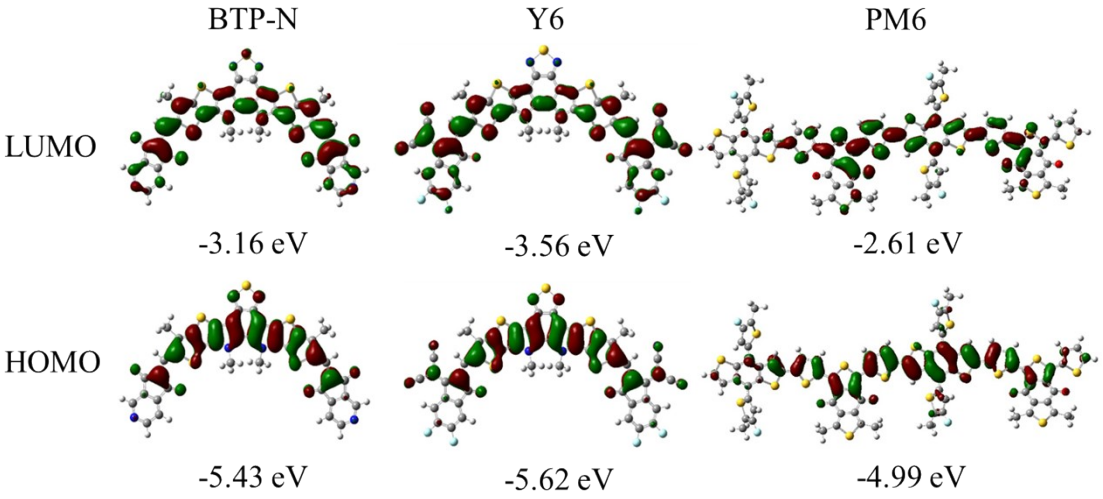

Figure S2. Frontier molecular orbitals obtained by the density functional theory (DFT) at the B3LYP/6-31G(d) level.

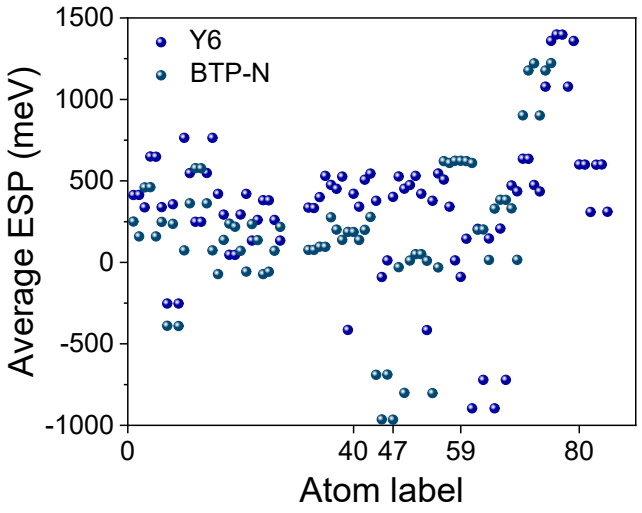

Figure S3. Average ESP values of atoms.

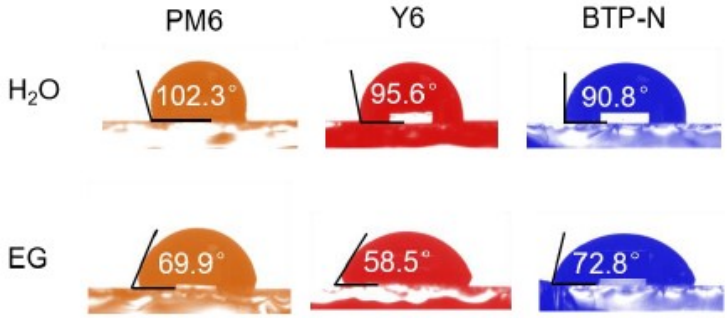

Figure S4. Contact angles of water and ethylene glycol on PM6, Y6, and BTP-N films.

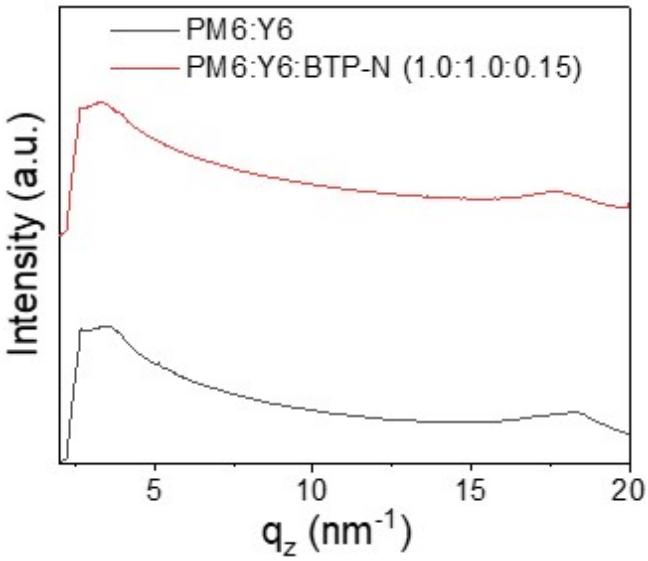

Figure S5. OOP line cuts for binary and ternary films.

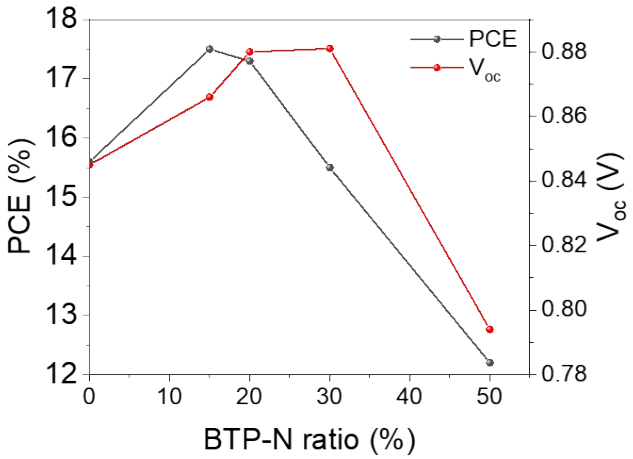

Figure S6. Variation of V_{oc} and *PCE* of ternary OSCs with different BTP-N contents.

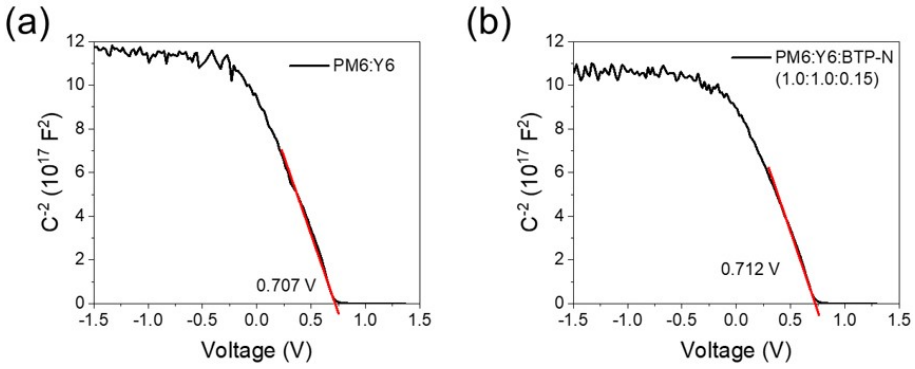

Figure S7. Mott-Schottky characteristics of devices based on (a) PM6:Y6 and (b) PM6:Y6:BTP-N (1.0:1.0:0.15).

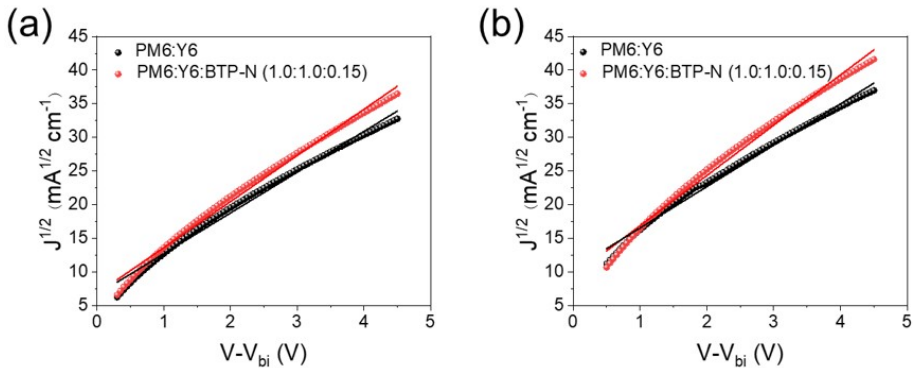

Figure S8. $J^{1/2}$-V fitting results of the hole-only (a) and electron-only (b) devices based on blend films measured by the SCLC method. The device structures for measurements of the hole and electron mobilities were ITO/PEDOT:PSS/active layer/MoO_3/Al and ITO/ZnO/active layer/PDINO/Al, respectively.

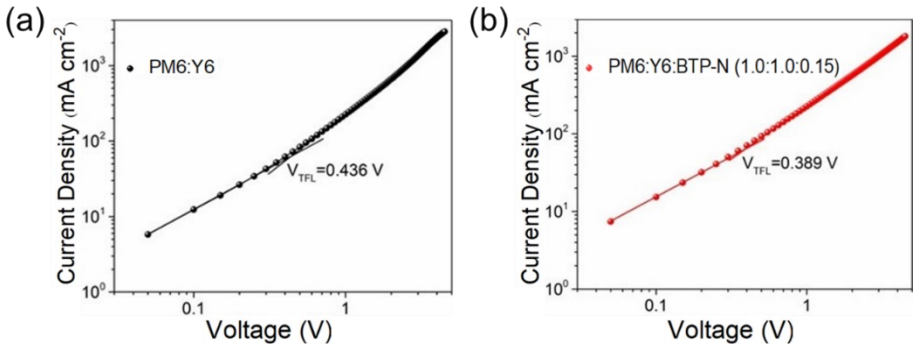

Figure S9. J-V characteristics of the electron-only devices based on (a) PM6:Y6 and (b) PM6:Y6:BTP-N (1.0:1.0:0.15) blend films.

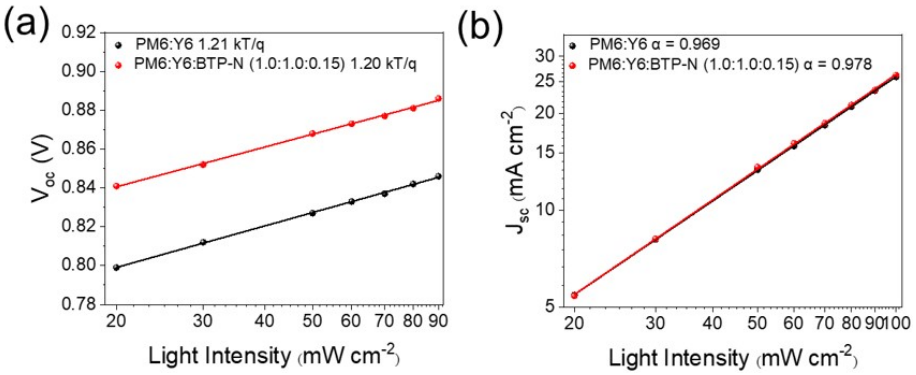

Figure S10. (a) V_{oc}-P_{light} and (b) J_{sc} -P_{light} curves of the optimized OSCs.

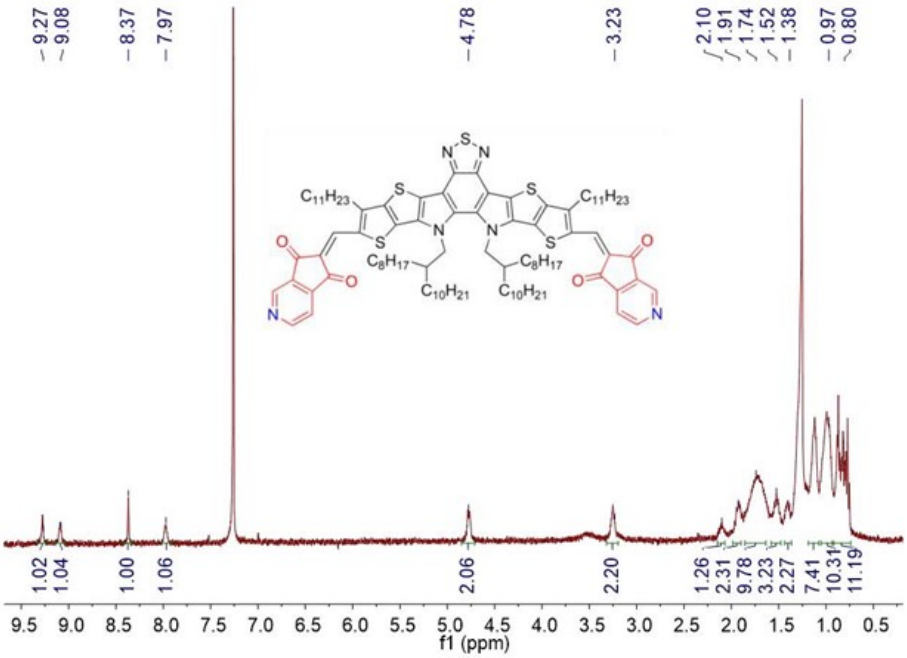

Figure S11. ^{1}H NMR spectrum of compound BTP-N.

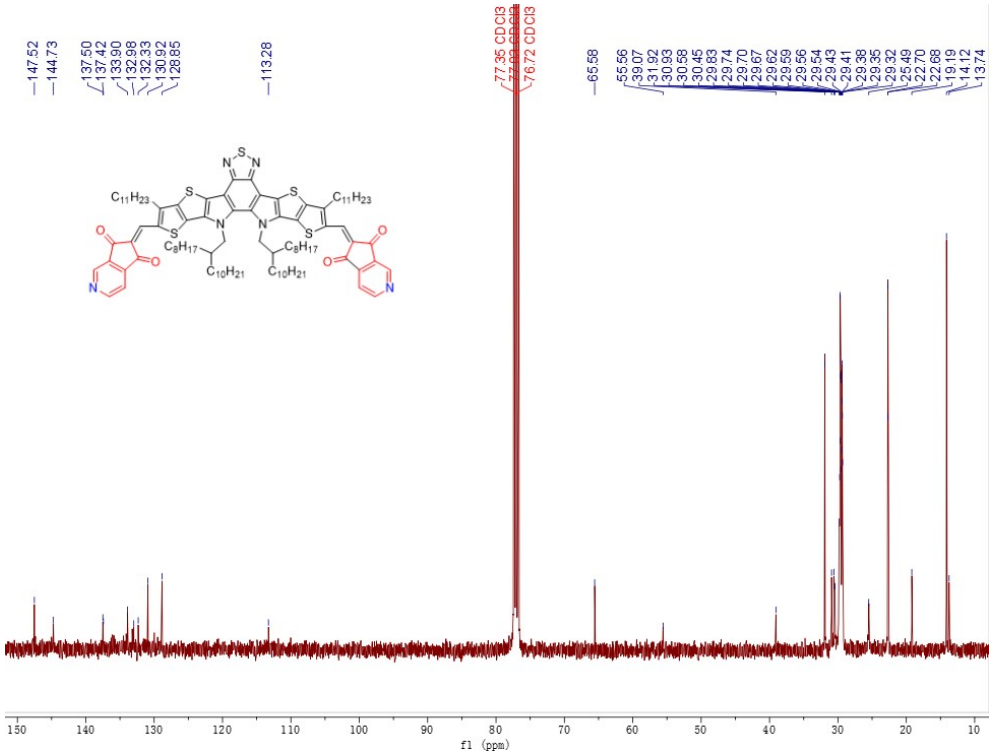

Figure S12. ^{13}C NMR spectrum of compound BTP-N.

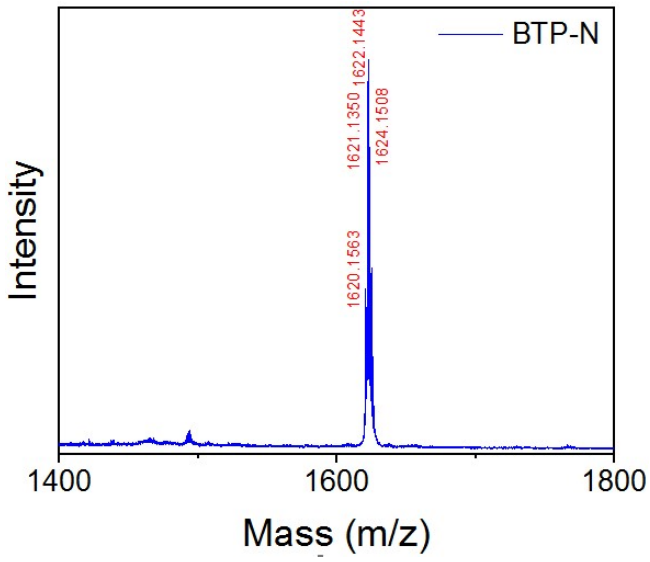

Figure S13. MALDI-TOF-MS spectrum of compound BTP-N.

Table S1. Maximal, minimal, and average ESP values, as well as molecular polarity index of PM6, Y6 and BTP-N.

Molecule	Average value (eV)	Minimal value (eV)	Maximal value (eV)	Molecular polarity index (eV)
BTP-N	0.12	-1.45	1.54	0.46
PM6	-0.03	-1.33	0.95	0.33
Y6	0.22	-1.45	1.72	0.51

Table S2. Performances of binary and ternary OSCs based on PM6:Y6 with different BTP-N contents.

PM6:Y6:BTP-N	V_{oc} (V)	J_{sc} (mA cm^{-2})	*FF* (%)	PCE (%)
1.0:1.2:0	0.845 (0.840 ± 0.006)	26.4 (26.4 ± 0.4)	70.0 (69.7 ± 0.5)	15.6 (15.3 ± 0.2)
1.0:1.0:0.15	0.866 (0.871 ± 0.014)	27.6 (27.4 ± 0.3)	73.4 (72.8 ± 0.8)	17.5 (17.2 ± 0.3)
1.0:1.0:0.20	0.880 (0.879 ± 0.003)	27.3 (27.3 ± 0.2)	72.3 (71.3 ± 0.8)	17.3 (17.0 ± 0.2)
1.0:1.0:0.30	0.881 (0.881 ± 0.003)	27.0 (26.7 ± 0.5)	65.3 (64.5 ± 0.9)	15.5 (15.1 ± 0.4)
1.0:1.0:0.50	0.794 (0.788 ± 0.010)	24.5 (24.7 ± 0.4)	62.8 (62.3 ± 1.1)	12.2 (11.7 ± 0.4)